

Elementary Response of Olfactory Receptor Neurons to Odorants

Vikas Bhandawat, Johannes Reisert and King-Wai Yau

Online Materials and Methods

Preparation. An adult frog (*Rana pipiens*) was chilled on ice and euthanized by rostral and caudal pithing. The olfactory epithelium was removed together with underlying bone from the nasal cavity and stored in normal Ringer at 4°C until use over a period of 24 hr. When needed, a small piece of epithelium was peeled from the bone and placed receptor-side up on cured Sylgard elastomer (184, Dow Corning) under normal Ringer. The cells were dissociated mechanically by repeatedly touching the epithelium with a razor blade. A 200- μ l volume of the Ringer containing the epithelial fragments/dissociated cells were transferred to a centrifuge tube, briefly triturated with a Pasteur pipette, and loaded into the recording chamber. The cells were allowed to settle for 30 min before bath perfusion started. They were viewed with DIC optics.

Suction-pipette recording and odorant application. The cell body of an isolated ORN was drawn into the tip of a glass suction pipette for recording membrane current, leaving the cilia exposed to bath solution (1,2). Typically, the dendrite of the cell retracted into the cell body, and about 75-80% (by visual inspection) of the surface of the rounded-up soma was drawn into the pipette; as a first approximation, the same percentage of the odorant-induced receptor current is expected to be recorded. The pipette was filled with normal Ringer and connected to a patch-clamp amplifier in current-recording mode. The membrane current was recorded on two channels, low-pass filtered at 20 Hz and 500 Hz (8-pole Bessel), respectively, in order to record the slow receptor current and the action potentials. All data analysis described here was carried out on the

20-Hz filtered recordings. The signals were digitized at 1 kHz. Single odorants were applied dissolved in either normal or 90% Ringer (see below). Solution changes were made by translating the interface between two solution streams across the recorded cell with a stepping motor attached to a three-barrel tubing (SF-77B, Warner Instruments). In some experiments, the time course of odorant application was monitored by using 90% Ringer containing the odorant, so that the solution change could be tracked by the resulting junction current (see, for example, Fig. 3b in paper). The half-maximal width of the displacement in the current recording due to junction current closely approximated (within 1 msec) the duration of the command pulse (assessed with low-pass filtering at 500 Hz). The reproducibility of the solution change was demonstrated by an absence of variance increase in repeated trials (Fig. 3b in paper, left upper panel; 20-Hz filtering). For technical reasons, we were limited to durations of odorant application greater than 20 msec. All numbers given in the text connected by “ \pm ” are mean \pm SD.

In experiments where the olfactory response was recorded in low-Ca²⁺ Ringer, the bath was typically switched to low-Ca²⁺ solution for 2 sec before the odorant pulse was applied, and then returned for at least 10 sec to normal Ringer after subsidence of the response before another odorant pulse was given to the cell. For experiments on quantal analysis, which involved a large number of weak stimuli, the above solution changes were shortened so that the duration between successive stimuli could be as short as 5 sec (see, for example, Fig. 2A in paper). When bath solution was switched to low-Ca²⁺ Ringer, a cell generally fired several action potentials and became quiescent afterwards; upon odorant stimulation, action potentials did not always appear. In normal Ringer, however, odorant stimulation typically elicited action potentials. Sometimes, an inward current appeared upon exposure of the cell to low-Ca²⁺ Ringer. This current appeared

to reflect constitutive transduction activity in some ORNs (unpublished observation). All results reported in the paper were from cells in which this current was absent.

Normal Ringer contained (in mM) 111 NaCl, 2.5 KCl, 1.6 MgCl₂, 1 CaCl₂, 0.01 Na-EDTA, 3 Na-HEPES, pH 7.7. Ringer with 20- μ M free Ca²⁺ and 2.6 mM free Mg²⁺ contained (in mM) 111 NaCl, 2.5 KCl, 3.5 MgCl₂, 0.1 CaCl₂, 1 nitrilotriacetic acid (NTA), 3 Na-HEPES, pH 7.7 (calculated according to the web-based program, MaxChelator). The total external divalent concentration was kept the same as in normal Ringer in order to minimize change in the extracellular blockage of the CNG channels by divalent cations. Ringer with 100 nM Ca²⁺ contained (in mM) 111 NaCl, 2.5 KCl, 2.6 MgCl₂, 0.6 CaCl₂, 1 EGTA, 3 Na-HEPES, pH 7.4; the lower pH was used in order to bring the pK_a of EGTA for Ca²⁺ within the usable range for achieving the desired free Ca²⁺ concentration. For the low-Ca²⁺ solution containing guanidinium, NaCl was replaced by guanidinium chloride, and titration was made with tetramethylammonium hydroxide instead of NaOH. 10 mM glucose was added to all solutions on the day of experiment. All recordings were done at room temperature (20-23°C)

Odorant solutions were made daily from pure stocks (Sigma). In most experiments involving a single odorant, cineole was used; otherwise, isoamylacetate was used. The conclusions were similar for both odorants. In experiments comparing the effects of two odorants on the same cell, cineole was compared to either isoamylacetate or acetophenone. Again, both pairings gave similar results. Altogether, close to 2,000 ORNs were studied. Of the three odorants, cineole was able to elicit responses from the largest number of cells (195 cells, *ca.* 10 %). Accordingly, very few cells were encountered that responded to each of two odorants (cineole/isoamylacetate or cineole/acetophenone). Odorant concentrations were 1 μ M to 2 mM. With the brief stimulus durations (e.g., 25 msec) that we used, we had to use higher

concentrations than generally reported in the literature, because the $K_{1/2}$ for eliciting a response depended strongly on the duration of odorant stimulation. We deliberately used very brief odorant pulses in order to focus on the “impulse response” of the cells (see also Supporting Online Material, section S1). In most of the experiments reported here, a cell was typically stable for ≥ 1 hr with little or no obvious decline in sensitivity.

Quantal and variance analyses. The approach was essentially the same as that previously described for analyzing single-photon responses in retinal rods (3). For quantal analysis of data collected in 100-nM Ca^{2+} solution, the individual responses to a series of identical odorant pulses were first averaged, and the averaged response waveform was fitted by a mathematical function representing the output of a series of 4 or 5 single-exponential low-pass filters. This function was then scaled to provide the least-squares fit to the individual responses, with the scaling factor representing the amplitude of each response. The experimental amplitude histogram was constructed based on these scaling factors. The ensemble variance (σ^2) and mean (m) values of the responses were calculated, on the other hand, directly from the raw responses (from their respective amplitude values at each digitized time point). The predicted Poisson distribution to be compared to the amplitude histogram was derived by first calculating $P_x = \lambda^x e^{-\lambda} / x!$, where $x = 1, 2, 3, \text{etc.}$ and $\lambda = m^2 / \sigma^2$, then plotting NP_x , where N is the total number of stimulus trials, against $x(\sigma^2/m)$. The predicted amplitude distribution was obtained by blurring the predicted Poisson distribution with a Gaussian of variance σ_0^2 , representing background noise, chosen to fit the 0-pA peak (failures) and a Gaussian of variance $(\sigma_0^2 + \sigma_1^2)$ chosen to fit the first non-zero peak in the histogram, where σ_1^2 represents the variance of the unitary response amplitude. The height of the first non-zero peak in the predicted distribution was scaled to fit the experimental

histogram based on the least-squares criterion. The Gaussians for the second, third and subsequent non-zero peaks were then automatically generated with variance $\sigma_0^2 + 2\sigma_1^2$, $\sigma_0^2 + 3\sigma_1^2$, etc. (see Eqn. 10 in 3) and heights constrained according to the likelihood of 2, 3, etc. events according to the Poisson distribution. For variance analysis of data collected in 20- μM Ca^{2+} solution, the same procedure was used, but the Gaussians were omitted by ignoring background variance and variance of the unitary response.

References

1. J. Reiser, H. R. Matthews, *J. Gen. Physiol.* **112**, 529 (1998).
2. G. Lowe, G. H. Gold, *J. Physiol.* **442**, 147 (1991).
3. D. A. Baylor, T. D. Lamb, K.-W. Yau, *J. Physiol.* **288**, 613 (1979).

Elementary Response of Olfactory Receptor Neurons to Odorants

Vikas Bhandawat, Johannes Reiser and King-Wai Yau

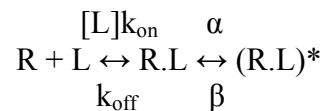
Supporting Online Material

S1. Relation between time course of active receptor and amplitude of the unitary response

Consider G-protein-coupled signaling as a chain of reactions leading from the activation of the membrane receptor, R, to the eventual effector signal (see, for example, 1). Let $r(t)$ denote the time course of the active state, R^* , of the receptor, and $h(t)$ denote the response function to an impulse of R^* . The response to the input function $r(t)$ is therefore given by the convolution integral of $r(t)$ and $h(t)$, or $\int [r(t') \times h(t-t')] dt'$. If $r(t)$ is very brief compared to $h(t)$, this integral simplifies to $[\int r(t') dt'] \times h(t)$. In other words, the amplitude of the response is simply proportional to the time-integrated receptor activity.

S2. Odorant dwell-time and the relation between odorant duration and response amplitude

To get a sense of how the odorant dwell-time is reflected by the relation between odorant duration and response amplitude, we adopt the following simple kinetic scheme for the activation of the odorant receptor protein:



Here R is the receptor, L is the odorant (ligand), R.L and (R.L)* are the inactive and active conformations of the liganded receptor complex, k_{on} and k_{off} are the binding and unbinding rate constants, [L] is the odorant concentration, and α , β are the forward and reverse rates for the transition to the active conformation. The probability of the liganded complex being in the

(R.L)* state is given by $\alpha/(\alpha+\beta)$, often referred to as the “efficacy” of a ligand. We need not include downstream steps in this working model because they are the same from cell to cell (essentially all involving G_{off} and type-III adenylyl cyclase, with very minor exceptions (2-4)).

Consider an odorant molecule that binds to a receptor molecule at time zero. Based on transition probabilities, the total lifetime of the active (R.L)* state, $\tau_{(\text{R.L})^*}$, before the odorant unbinds can be calculated to be $(\alpha/\beta)k_{\text{off}}^{-1}$. Likewise, the total lifetime of the inactive R.L state is given by k_{off}^{-1} . Thus, the total odorant dwell-time is given by $\tau_{(\text{R.L})^*} + \tau_{\text{R.L}} = k_{\text{off}}^{-1}(\alpha/\beta + 1)$. This expression is the same as the mean burst time derived for a ligand-gated channel (5).

Next, consider an odorant applied as a square pulse of duration T, where T is much shorter than the time course of the response so that the stimulus approximates a delta-function and the response is effectively an “impulse response” (see 6). In addition, if the odorant dwell-time is not a dominant time constant for the response waveform (see text in paper), the response amplitude in the linear range of the dose-response relation (i.e., no non-linear response compression due to downstream steps) is simply proportional to the time-integrated receptor activity (see previous section), A_R , given by:

$$\int (\text{R.L})^* dt = \int_0^T f(t) dt + f(T) \int_0^{\infty} g(t') dt'$$

where $f(t)$ is the fraction of R in the (R.L)* state at time t after the start of the odorant pulse, and $g(t')$ is the decay time course of $f(T)$ after the removal of L (t' designates the time lapsed after odorant removal).

We have carried out extensive calculations with different relative values of $[L]k_{\text{on}}$, k_{off} , α , and β . For this purpose, we adopted the normalized parameters $\alpha/k_{\text{off}} = A$, $\beta/k_{\text{off}} = B$, and $[L]k_{\text{on}}/k_{\text{off}} = C$. We then evaluated the response amplitude ($\propto A_R$) using various values of A/B

(0.01, 0.1, 1 and 10) together with A values ranging from 10^{-3} to 10^4 and C values ranging from 0.1 to 10. Probably not all of these values are realistic, but they are instructive in showing how A_R behaves overall. The A/B ratio is a measure of the efficacy (given by $1/[1+B/A]$), while the absolute values of A and B indicate the speed of the transitions between R.L and (R.L)* relative to the odorant unbinding rate. Finally, the value of C represents the on-rate in relation to the off-rate for a given odorant concentration.

Fig. S1-S3 are examples of the calculated response amplitude as a function of the normalized odorant duration variable T^\wedge , where $T^\wedge = T \cdot k_{\text{off}}$. It can be seen that, in general, the relation approaches asymptotically to a linear relation, with an extrapolated time intercept corresponding to $-\Delta T^\wedge$. The most relevant cases are with $C \gg 1$ (say, equal to 10), corresponding to a high odorant concentration such that the receptors are saturated by binding. In these cases, $-\Delta T^\wedge$ is the effective dwell time of the odorant after its removal from the solution, given by $A/B + 1 + B^{-1} [A/(A + B)]$, or, in unnormalized parameters, $k_{\text{off}}^{-1} (\alpha/\beta + 1) + \beta^{-1} [\alpha/(\alpha + \beta)]$. This odorant dwell-time is very similar to that derived above, except for the extra term $\beta^{-1} [\alpha/(\alpha + \beta)]$, which arises because the asymptotic linear relation corresponds to the situation in which a fraction $\alpha/(\alpha + \beta)$ of the receptors is already in the (R.L)* state at the end of the odorant pulse T.

Fig. S4 provides an intuitive approach of the same problem, making use of the simple situation where $\alpha, \beta \gg k_{\text{on}}, k_{\text{off}}$. The left panel shows the time dependence of the (R.L)* state due to an odorant pulse, for two hypothetical cases where the ligand unbinds quickly (red) and slowly (black), respectively. In either case, the receptors are rapidly saturated (though not all are in the active state, (R.L)*) at high concentration of odorant. The right panel shows the corresponding relations between response amplitude and stimulus duration. The response

amplitude is proportional to the total time the receptor spends in the active state, if the experiments are done in the linear regime of the dose-response relation. This total time is given by the time-integral under $(R.L)^*(t)$, given by $(T + \tau_{\text{off}})$, where T is the stimulus duration and τ_{off} is the odorant dwell-time. The duration-response relation is a linear relation that intersect the time-axis at a value equal to $-\tau_{\text{off}}$.

S3. “Efficacy” of photoisomerized rhodopsin versus efficacy of receptor-odorant complex

Photoisomerized rhodopsin has a high efficacy of near unity, because the equilibrium between the inactive meta-I state and the active meta-II state of photoisomerized rhodopsin strongly favors the active state, see 7). By contrast, for the ORN in Fig. 4a of the paper, the efficacy of acetophenone would at most be $1/14 = 0.07$ even if cineole had an efficacy of unity; however, it is mostly unlikely that cineole would have an efficacy of unity because this would have led to a very long odorant dwell-time for cineole (see kinetic scheme in previous section here).

S4. Probability of missing the most sensitive receptors in our experiments

We have recorded from close to 2,000 ORNs overall, of which 195 cells (about 10%) responded to cineole. Assuming, for simplicity, roughly equal distributions of receptor proteins among ORNs, we may conclude that about 10% of all receptor proteins responded to cineole. From 65 of the 195 cells, the $K_{1/2}$ for a 500-msec cineole stimulus (the longest duration used) was 1-500 μM ($131 \pm 142 \mu\text{M}$). In another 98 cells with the same cineole stimulus, $K_{1/2}$ was $>100 \mu\text{M}$ but not determined exactly. In a previous study with identical conditions by one of us (8), 6 of the 9 most sensitive cells out of >180 cineole-responsive ORNs gave $K_{1/2}$ values of 3-8

μM with a 1-sec stimulus (the remaining 3 cells gave lower, but undetermined, $K_{1/2}$ values). Thus, a $K_{1/2} \sim 1 \mu\text{M}$ (500-msec stimulus) may correspond to the highest sensitivity to cineole. Furthermore, the total number of cineole-responsive cells for which we have information about $K_{1/2}$ is >343 .

There is no published report of the number of odorant receptor species in adult frog. A study (9) on tadpoles of *Xenopus laevis* indicates that their ventral main olfactory bulb has about 230 glomeruli and receives projections from water-nose receptor cells (i.e., receptors to water-soluble odorants). The dorsal main olfactory bulb has no clearly defined glomeruli; possibly it normally receives projections from receptor cells to volatile odorants, but the latter are not yet mature because the tadpoles live continuously under water. For simplicity, we assume that approximately the same number of glomeruli would develop in the dorsal main olfactory bulb in the adult frog. We further assume that, as in mouse, olfactory receptor neurons expressing the same receptor protein project largely to two glomeruli. With this reasoning, the total number of odorant receptor species would be $2 \times 230/2 \sim 300$. Obviously, this number is very rough.

If there are 300 receptor proteins in adult frog, the number of cineole-responsive receptor proteins will be *ca.* 30 (i.e., $\sim 10\%$). Thus, the probability that we could have missed, after measuring sensitivity from > 343 cineole-responsive cells, any receptor among the pool of 30 cineole-sensitive receptor proteins is less than $0.97^{343} = 2.9 \times 10^{-5}$, which is very low indeed. If there are 500 receptor types, the probability of missing any one cineole-responsive receptor will be less than $0.98^{343} = 9.8 \times 10^{-4}$. Even if there were as many as 1,000 receptor types in frog as in mouse, the probability of missing any one cineole-responsive receptor would still be less than $0.99^{343} = 0.03$, which is quite small.

References

1. M. G. Fuortes, A. L. Hodgkin, *J. Physiol.* **172**, 239 (1964).
2. D. M. Juilfs *et al.*, *Proc. Natl. Acad. Sci. USA.* **94**, 3388 (1997).
3. M. R. Meyer, A. Angele, E. Kremmer, U. B. Kaupp, F. Muller, *Proc. Natl. Acad. Sci. USA.* **97**, 10595 (2000).
4. W. Lin, J. Arellano, B. Slotnick, D. Restrepo, *J. Neurosci.* **24**, 3703 (2004).
5. D. Colquhoun, A. G. Hawkes, *Proc. R. Soc. Lond. B* **211**, 205 (1981).
6. D. A. Baylor, A. L. Hodgkin, *J. Physiol.* **234**, 163 (1973).
7. H. Imai, T. Mizukami, Y. Imamoto, Y. Shichida, *Biochemistry* **33**, 14351 (1994).
8. J. Reisert, H. R. Matthews, *J. Physiol.* **519**, 801 (1999).
9. L. P. Nezhlin, D. Schild, *Cell Tissue Res.* **302**, 21 (2000).

Figure Legends

Figure S1. Calculated dependence of olfactory response amplitude on the duration of odorant stimulation under the condition of high odorant concentration ($C = [L]k_{on}/k_{off} = 10$). See Section S2 in text. Each panel represents a different A/B ratios ($A = \alpha/k_{off}$, $B = \beta/k_{off}$). Within each panel, different values of A and B have been chosen. The x-intercept gives the dwell-time of the odorant on the receptor.

Figure S2. Calculated dependence of olfactory response amplitude on the duration of odorant stimulation under the condition of $C = [L]k_{on}/k_{off} = 1$. Otherwise, this figure has the same format

as Fig. S1. Unlike the situation in Fig. S1, the x-intercept here does not necessarily correspond to the odorant dwell-time because C is not high enough.

Figure S3. Calculated dependence of olfactory response amplitude on the duration of odorant stimulation under the condition of $C = [L]k_{on}/k_{off} = 0.2$, i.e., less than one. Otherwise same format as in Fig. S1 and S2. Because C is relatively small, the x-intercept bears even less correlation to the odorant dwell-time.

Fig S4. A schematic diagram, just for illustration purposes, showing how odorant dwell-time affects the relation between response amplitude and odorant duration in the linear range.

Left panel: time course of the active receptor-odorant complex upon exposing an olfactory receptor cell to a high odorant concentration for duration T , under the two extreme cases of weak binding (black) and strong (red) binding, respectively. Right panel: Corresponding relations between response amplitude and T in the linear range. The x-intercept of the duration-response relation is a measure of the dwell-time.

C=10

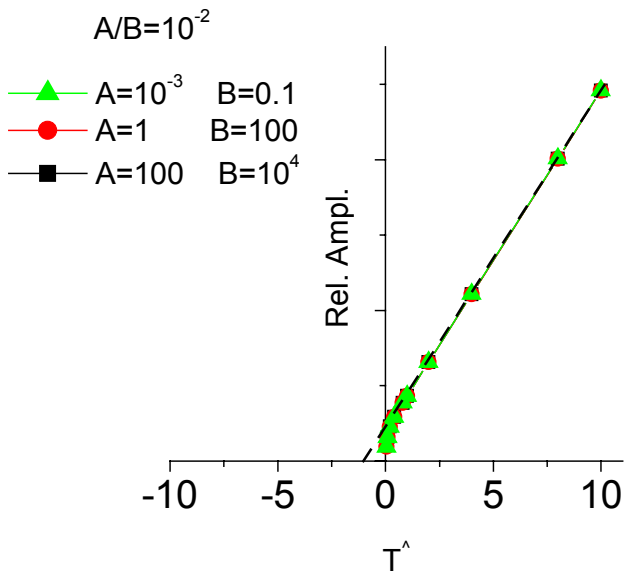
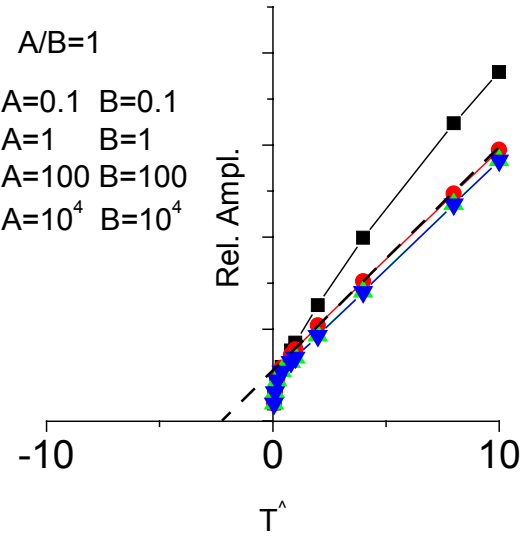
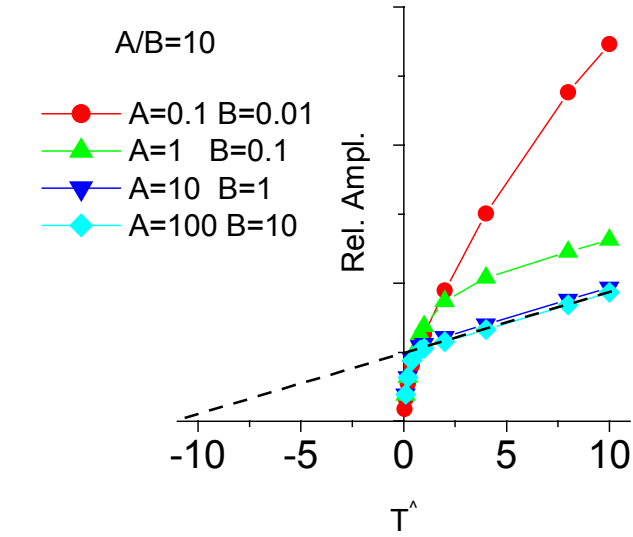


Fig. s1

C=1

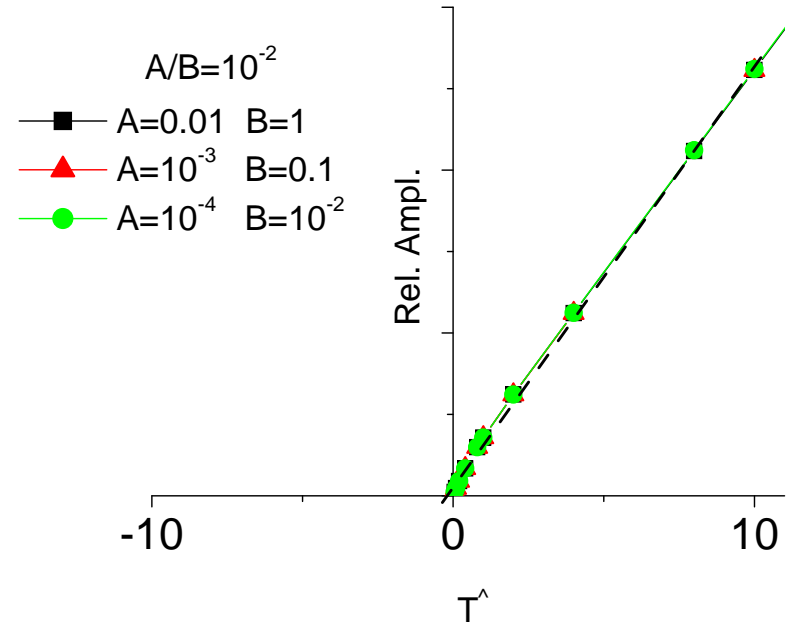
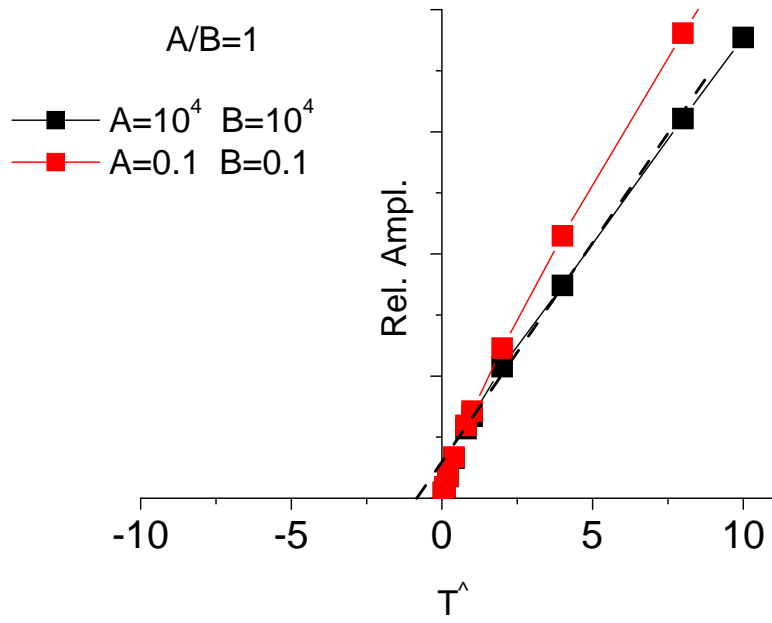


Fig s2

C=0.2

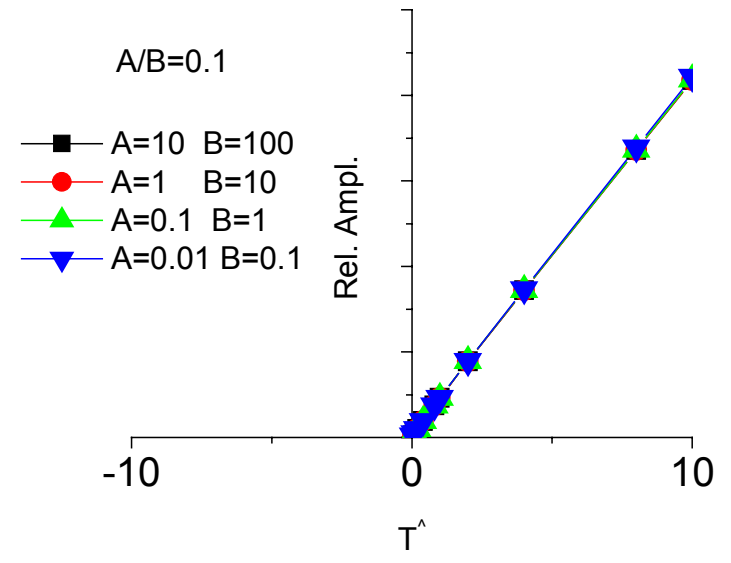
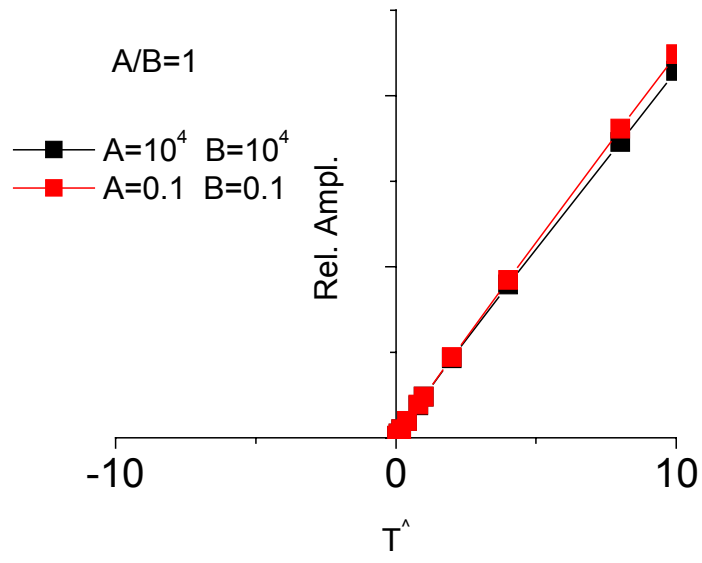


Fig s3

